

Prestressed CFRP for structural strengthening

Julien Michels¹, Christoph Czaderski¹, and Masoud Motavalli^{1,2}

¹ Empa, Dübendorf, Switzerland

² University of Tehran, Tehran, Iran

ABSTRACT: Nowadays an increasing number of existing constructions, due to their ageing and new safety standards, require structural repair. In this context, carbon fiber reinforced polymers (CFRP) offer considerable advantages. Beside their high tensile strength (above 2000 MPa), they allow an easy installation on construction site because of their low density. Furthermore, the absence of corrosion effects enhances the applicability for long-term resistance.

In order to benefit from the material's elevated strength in tension, prestressing seems an adequate and useful approach. At the Swiss Federal Laboratories for Materials Science and Technology (Empa), a non-mechanical anchorage technique was developed with the goal to avoid any steel pieces for anchoring. The 'gradient anchorage method' foresees epoxy adhesives to guarantee bond between concrete and reinforcement. Towards the strip ends, the prestressing force is continuously decreased to zero with intermediate adhesive curing.

In the present paper, a calculation method based on ordinary cross section analysis is presented. The method delivers the compression strains in the concrete, the tensile strain in the steel and CFRP reinforcement as well as the load-displacement curves and the mean bond shear stresses between the CFRP strips and the concrete. The numerical results are compared to experimental data. In general, a good concordance between experiments and calculations can be observed.

1 INTRODUCTION

Carbon Fiber Reinforced Polymer (CFRP) strips have become a popular technique for structural strengthening. High stiffness, high tensile strength combined with a very low density and no corrosion effects render this material highly efficient for repairing existing civil structures. In order to fully use the material's strength, prestressing seems to be a possible way to avoid debonding phenomena resulting in a tensile failure of the external reinforcement. At Empa, the 'gradient method' for anchoring the strip at the beam end in case of prestressing was developed and presented amongst others in Meier & Stöcklin (2005), Czaderski & Motavalli (2006) and Aram et al. (2008). This anchorage method consists in a gradual force release at the strip end with intermediate accelerated adhesive curing (Czaderski et al, (2010)). Eventually, the initial prestressing force is completely set to zero at the strip end.

In the present paper, a test series of four RC beams (firstly presented in Meier & Stöcklin (2005)) without, with passive as well as with prestressed CFRP strips subjected to static loading are presented. A certain number of observations out of the experimental results are presented

and commented. Simultaneously a calculation technique for ordinary cross section analysis is presented and the numerical results are compared with the experimental data.

2 CALCULATION METHOD

2.1 Constitutive material laws

The used constitutive material laws are presented in

Figure 1. In uniaxial tension, concrete is defined throughout a linear-elastic stress-strain law up to its tensile strength f_{ct} . Afterwards, no softening behavior is taken into account. In uniaxial compression, a Hognestad parabola according to Oztekin et al. (2003) is applied. A linear elastic (σ, ε)-relation until yielding followed by a linear hardening up to failure is used to describe the steel reinforcement's behavior under both tension and compression loading. Eventually, the CFRP reinforcement is taken into account with a linear-elastic behavior in tension up to the tensile strength $f_{u,CFRP}$. For the numerical iteration, material parameters are used as given in Meier & Stöcklin (2005) and Kotynia et al. (2010). Uniaxial tensile strength is derived from the uniaxial compressive strength f_c according to Muttoni (2003).

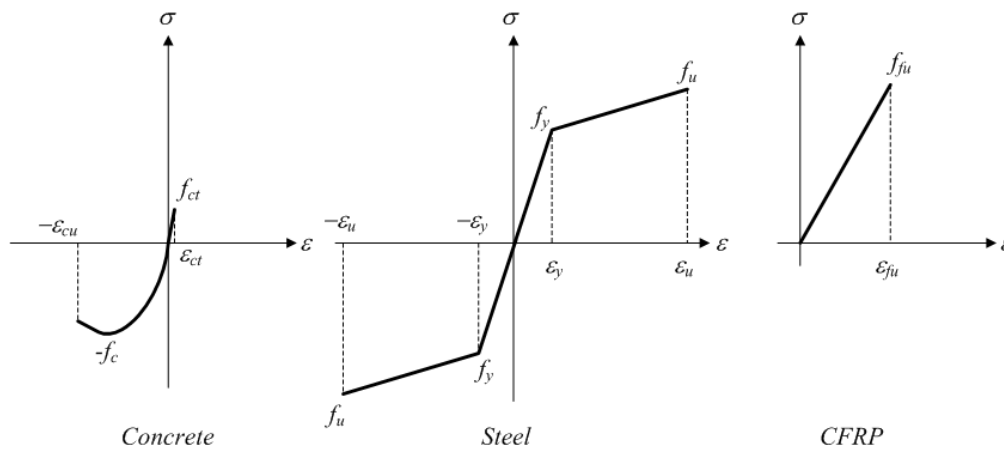


Figure 1. Constitutive stress-strain laws for concrete, steel and CFRP

2.2 Cross Section Analysis

Figure 2 presents the strain and stress distribution for both un-prestressed and prestressed beams. The equilibrium in the cross section is established by an automatised iterational process. For a given concrete compressive strain in the upper top fibre, the height of the compressive zone, using the usual assumption that the cross-section remains plane and normal to the neutral axis, is iterated until a force equilibrium ($\Delta F=0$) between compressive and tensile forces is obtained (see (1)).

$$F_c + F_{s'} = F_{ct} + F_s + F_f \quad (1)$$

With: F_c =compression force in the concrete compressive zone, $F_{s'}$ =compression force in the upper steel reinforcement, F_{ct} =tensile force in the concrete in the tensile zone, F_s =tensile force in the lower steel reinforcement, F_f =tensile force in the CFRP strip

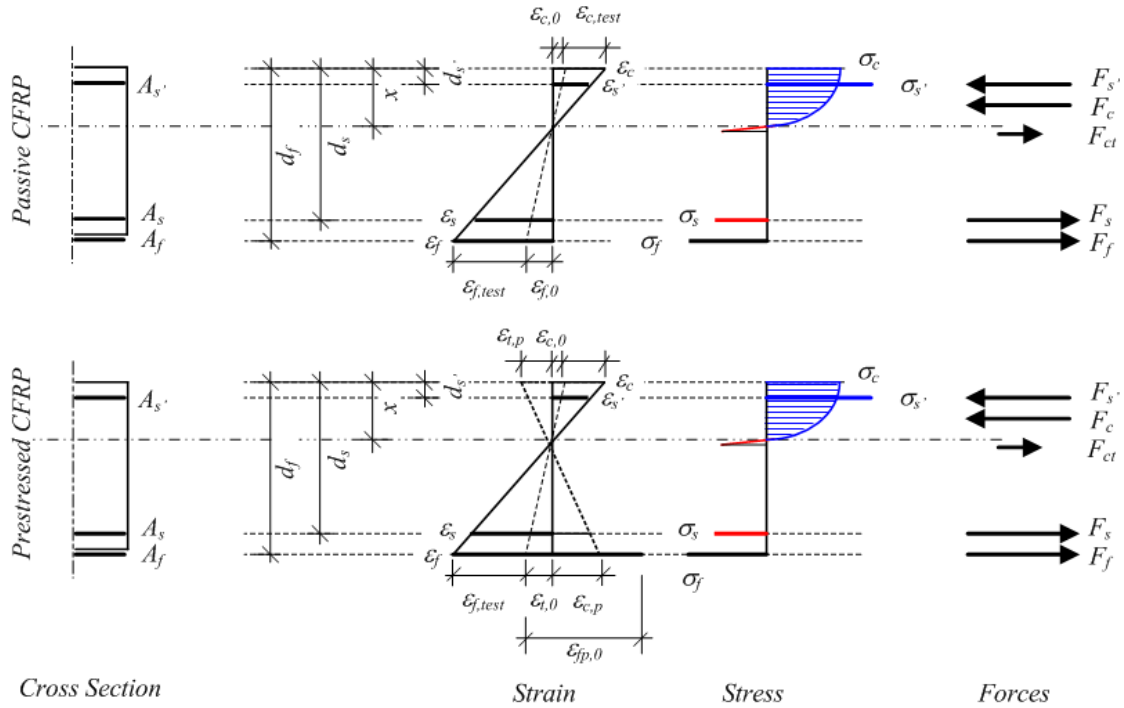


Figure 2. Strain and stress distribution in the cross section with non-prestressed (passive) and prestressed CFRP reinforcement

2.3 Deflection and bond stress calculation

The deflection values of the beam can be obtained by a double integration of the cross-sectional curvature χ , as defined in (2) (beam rotation ϕ) and (3) (deflection w).

$$\phi = \int_0^L \chi \cdot dx \quad (2)$$

$$w = \int_0^L \phi \cdot dx \quad (3)$$

With: ϕ =beam rotation, w =deflection, L =span length, χ =curvature

The developed calculation tool also allows to obtain the mean interfacial shear stress (equivalent to the force difference within the CFRP strip over a certain axis distance), the CFRP and steel strain at different load levels over the beam axis. It is pointed out that the mentioned anchorage gradient is not taken into account into the calculation. The mean interfacial bond stress τ is obtained by evaluating the force change in one CFRP strip over a plate segment Δx (4).

$$\tau = \frac{\Delta F_f}{n_f \cdot b_f \cdot \Delta x} \quad (4)$$

With: ΔF_f =total force in the CFRP strips, n_f =number of CFRP strips, b_f =width of the CFRP strip, Δx =plate segment

(3)

3 EXPERIMENTAL INVESTIGATION, RESULTS AND COMPARISON WITH CALCULATION VALUES

3.1 Test setup and plate specimens

The test setup by Meier and Stöcklin (2005) is shown in Figure 3. In total, 4 reinforced concrete plates with a cross-section of 1000 x 220 mm and a total span L of 6 m were submitted to 6-point loading with four equal forces distributed over the specimen length. The reference plate T1 was only reinforced with internal 7Ø8mm upper compressive and 7Ø12mm lower tensile reinforcement. In order to evaluate the beneficial effects of both non-prestressed and prestressed CFRP strengthening, three additional tests were carried out. On beam T2, two passive CFRP strips with a width b_f of 50 mm and a thickness t_f of 1.24 mm were installed. Beam T3, with the same strip type and quantity than the previous one, was prestressed up to a CFRP strain level of approximately 5.92 ‰ (0.00592), which corresponds to an initial CFRP stress of 977 MPa. The last specimen T4 was also prestressed, but with a total number of 4 strips of 50 mm width and a reduced thickness t_f of 0.61 mm (same total CFRP cross-sectional area than T3 and T2!) prestressed up to a strain level of 6.5 ‰ (0.0065), equivalent to an initial stress of 969 MPa.

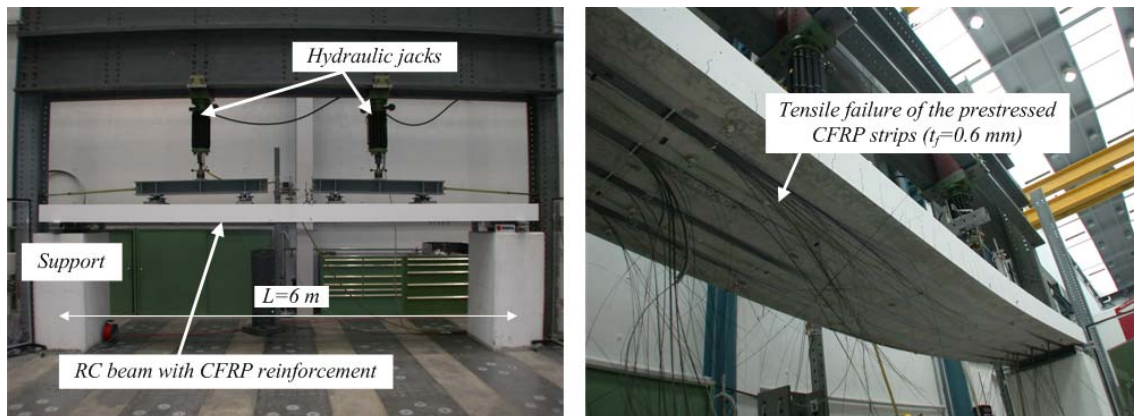


Figure 3. Experimental test setup and failure mode of test T4

3.2 Experimental and numerical results

In Figure 4, the total force $4F$ is plotted against the mid-span deflection for both the experimental and calculation (CSA), whereas Figure 5 shows the compressive upper strain in the concrete as well as the tensile strain in the CFRP reinforcement at midspan for the plates T2, T3 and T4 (in the tensile region, a DMS was installed on each strip, thus 2 curves are shown for T2 and T3 and 4 curves for T4).

In comparison to the reference girder T1, the passive CFRP reinforcement of specimen T2 does not offer any advantages regarding the cracking load. However, one can easily observe an enhancement in the ultimate load of 38 % (72 kN to 99 kN). On the other hand, both prestressed beams show a much stiffer behaviour together with a higher cracking load in the range of 30 kN in comparison to about 10 kN for the non-prestressed specimens. Furthermore, the ultimate load is enhanced, too (134 kN for T3 (enhancement of 86 %) and 137 kN for T4 (enhancement of 90 %)). As it could be observed during the tests, specimen T2 failed by strip debonding without attaining the CFRP's maximum tensile strength. The same failure type could be observed for the plate T3. By enlarging the CFRP width and reducing strip the thickness for T4 and thus

reducing the interfacial concrete-CFRP shear stresses, a CFRP tensile failure could be observed, indeed.

In general, the numerical calculations approximate the experimental results well. For all plates, the cracking load can be obtained precisely. As no tension stiffening is included in the numerical model, the experimental and numerical force-deflection curves differ slightly. As pure cross-section analysis offers the total bearing capacity up to tensile failure of the CFRP reinforcement, the ultimate load of T2 is overestimated with the numerical predictions. As premature debonding failure occurs, the material (CFRP) is not able to develop its full strength capacities. Similar to T2, plate T3 also fails in debonding. For the latter however, the CFRP strips were very close to tensile failure. Hence, with regard to the calculation values assuming a tensile failure of the CFRP, there is almost no overestimating of the total bearing capacity.

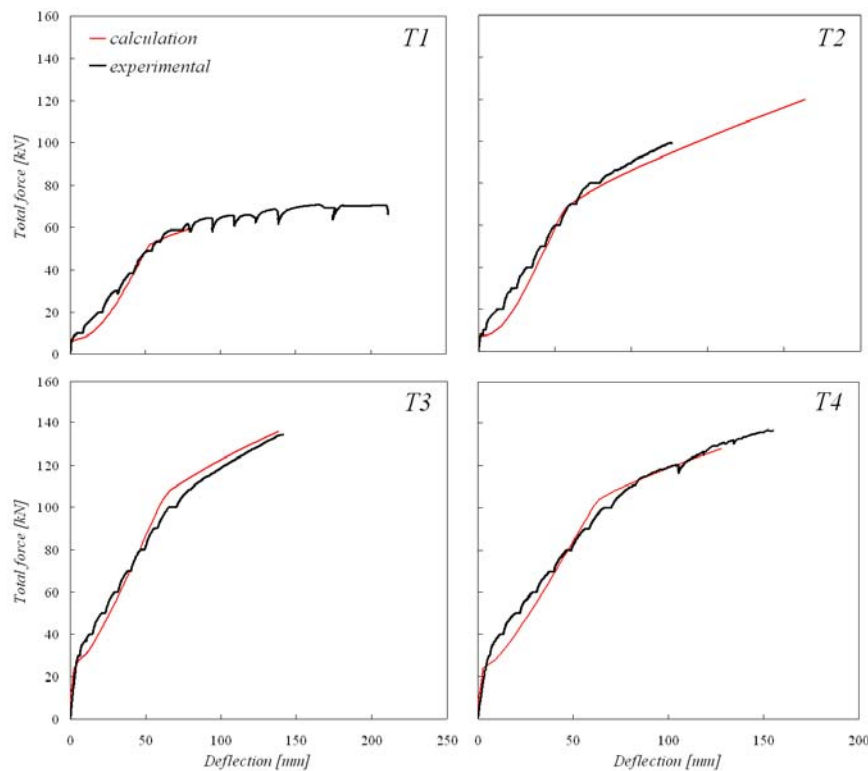


Figure 4. Experimental and numerical force-deflection curves for the plates T1, T2, T3 and T4

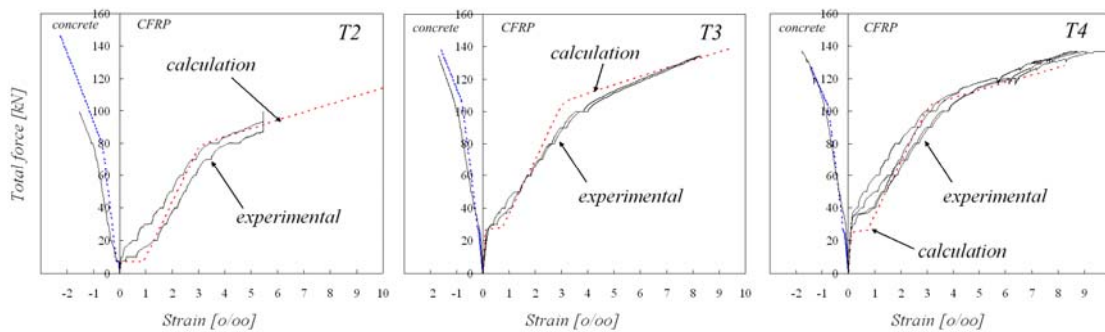


Figure 5. Force-strain (compressive for concrete and tensile for CFRP) curves at midspan for the plate specimens T2, T3 and T4

For half the span length L , Figure 6 presents curvature, interfacial bond stress, CFRP strain and steel strain for total loading forces $4F$ of 100 kN (failure load of T2) and for failure levels of T3 and T4.

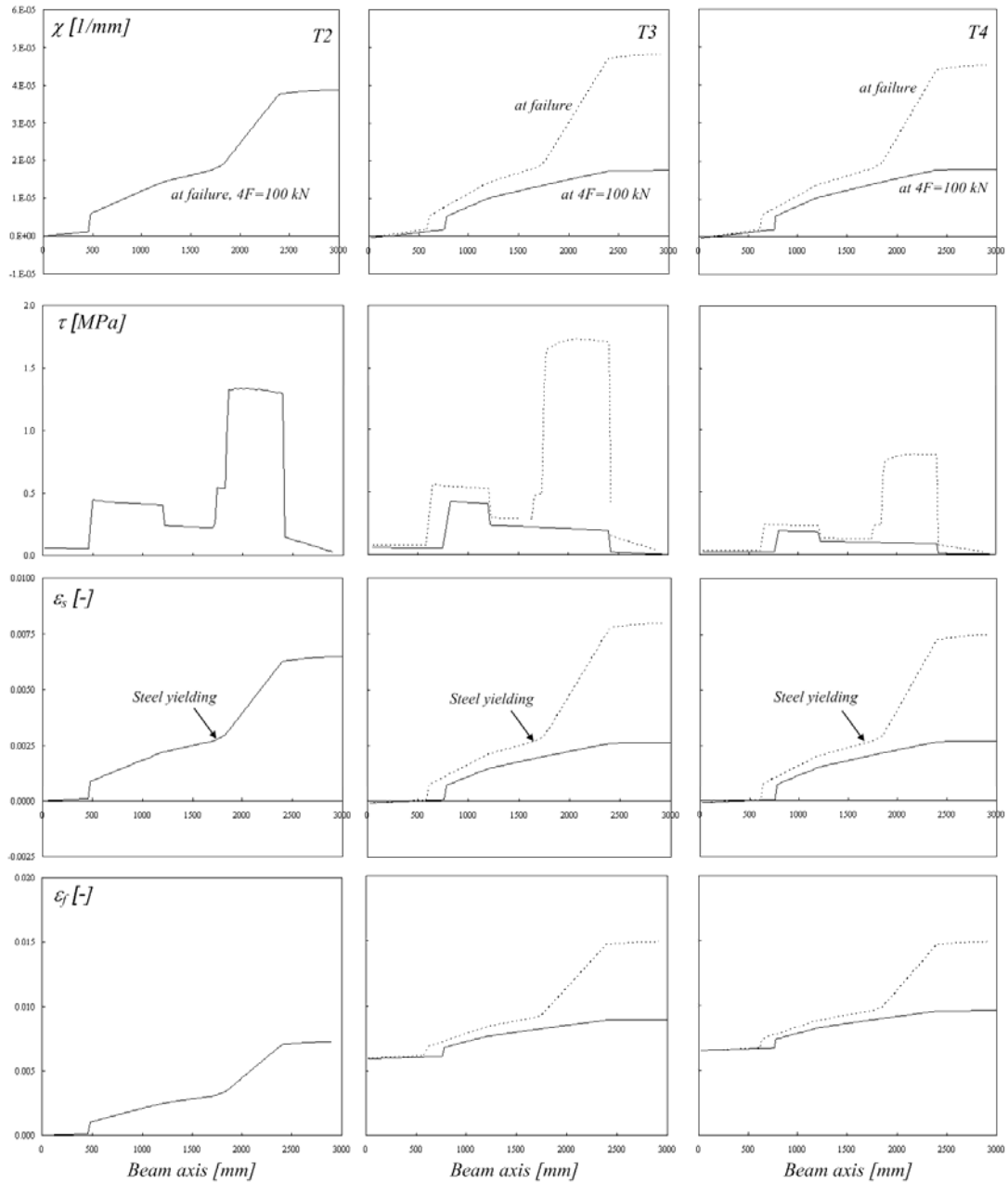


Figure 6. Curvature, interfacial shear stress, steel strain and CFRP strain of plates T2, T3 and T4 at $4F=100$ kN and at failure level along the plate axis (from $x=0$ to $x=L/2$)

4 DISCUSSION

A first comparison reveals clearly higher shear stresses τ for the non-prestressed beam T2 compared to the prestressed specimen T3 at the same load level ($4F=100$ kN). Hence, the prestressing offers a beneficial effect by lowering the concrete-CFRP interface stresses and thus allowing to take further advantage of the CFRP strip strength reserve. This reduction in shear stresses is due to an absence of steel yielding at a lower load level of $4F=100$ kN. With further loading however, the plate T3 also reaches the shear stress level previously attended by the passively strengthened plate. By increasing the number of CFRP strips from two to four and simultaneously reducing the strip thickness to 0.61 mm, the total area in CFRP reinforcement and thus the theoretical total bearing capacity are kept constant. However, due to the better shear stress distribution (four strips instead of two), debonding is avoided and one can use the strengthening material in a more efficient way.

5 PARAMETER STUDY

Figure 7 presents a parametrical study on the effect of different prestress levels on the moment-curvature relation as well as on the distribution of the interfacial shear stresses along the beam axis at failure. It becomes evident that a higher prestress level of the CFRP strip results in a higher structural stiffness and a higher cracking moment. Conjointly, as it can be observed in the right diagram from Figure 7, that higher prestressing results in a lower interfacial bond stress and a shorter length of higher shear stresses thus reduces the risk of debonding. However, one has to consider the fact that a stiffer structural behaviour reduces the ductility of the structural element. As an example, the fib-bulletin 14 (2001) suggests a curvature χ_u at ultimate load state being 1.7 or 2.6 times (depending on the concrete compressive strength) higher than the curvature χ_y at steel yielding. With regard to our strength range (approx. 45 MPa), prestressing up to only 6 ‰ would be tolerated.

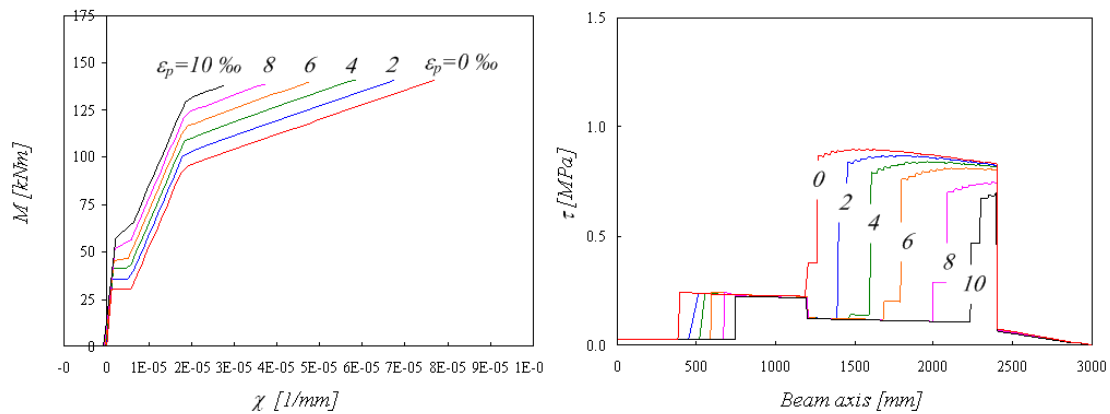


Figure 7. Moment-curvature and shear stress distribution from $x=0$ to $L/2$ at failure level for different prestress levels (remaining geometry parameters identical to the previous plates by Meier and Stöcklin (2005))

6 CONCLUSIONS

The presented experimental and numerical results allow to draw a certain number of conclusions. The plate tests shows that a RC plate reinforced with CFRP presents a higher total bearing capacity than the reference girder. In addition, the fact of prestressing the CFRP reinforcement including the used anchoring method is gainful with regard to the cracking load as well as to the ultimate load. Furthermore, prestressing reduces the interfacial bond stresses between the concrete and CFRP strip and thus delays a possible debonding failure. By increasing the bond surface between the two structural components, shear stresses are even further reduced and it is possible to obtain a more defined failure mode with tensile failure of the CFRP strip(s). Numerical cross-section analysis predicts the experimental observations in a satisfactory way. Referring to cracking load, ultimate load and interfacial bond stress, prestressing of the CFRP strip has beneficial effects and the reinforcing material can be fully exploited. Limitations for the prestressing level are set due to ductility conditions required by design codes.

REFERENCES

- Aram, MR, Czaderski, C, and Motavalli, M. 2008. Effects of Gradually Anchored Prestressed CFRP Strips Bonded on Prestressed Concrete beams, *Journal of Composites for Construction*, ASCE, 12: 25-34.
- Czaderski, C, and Motavalli, M. 2007. 40-year-old full-scale concrete bridge girder strengthened with prestressed CFRP plates anchored using gradient method, *Composites Part B: Engineering*, 38: 878-886.
- Czaderski C, Martinelli, E, Michels, J, and Motavalli, M., 2010. Effect of curing temperature and curing duration on strength development in a commercial epoxy resin utilized for structural strengthening *International Journal of Adhesion and Adhesives*, submitted for consideration for publication.
- fib* – Bulletin 14, 2001. Externally bonded FRP reinforcement for RC structures
- Kotynia, R, Walendziak R, Stoecklin I, and Meier, U. 2010. RC slabs strengthened with prestressed and gradually anchored CFRP strips under monotonic and cyclic loading, *Journal of Composites for Construction*, ASCE, accepted for publication.
- Meier, U and Stöcklin, Y. 2005. A Novel Carbon Fiber Reinforced Polymer (CFRP) System for Post-Strengthening, International Conference on Concrete Repair, Rehabilitation and Retrofitting (ICCRRR), Cape Town, South Africa.
- Muttoni, A. 2002. Conception et dimensionnement des elements de structures, Lecture on reinforced concrete, École Polytechnique Fédérale de Lausanne (EPFL).
- Oztekin, E, Pul, S, and Husem, M. 2003. Determination of rectangular stress block parameters for high performance concrete, *Engineering Structures*, 25: 371-376.